CrossMark

ORIGINAL PAPER

A study on the role of land-atmosphere coupling on the south Asian monsoon climate variability using a regional climate model

C. K. Unnikrishnan[1] · M. Rajeevan[2] · S. Vijaya Bhaskara Rao[3]

Abstract Land-atmosphere coupling over the south Asian monsoon region is examined using a regional climate model. For this purpose, the Weather Research and Forecasting (WRF) model with a resolution of 45 km was used. In the control experiment (CTL), the model was integrated from the year 2000 to 2011 and allowed the soil moisture interaction with the atmosphere using a coupled land surface model. In the second experiment (CSM), the soil moisture evolution at each time step was replaced with the climatology of soil moisture taken from the control run. The results reveal that land-atmosphere coupling plays a critical role in influencing the south Asian monsoon climate variability. Soil moisture is found to have stronger impacts on daily maximum temperature compared to minimum temperature. Soil moisture also makes a significant contribution to monsoon rainfall variability over the monsoon region. The coupling strength for large-scale rainfall is found to be higher compared to that of cumulus rainfall. Soil moisture is found more strongly coupled to sensible heat flux over most of the monsoon region.

1 Introduction

The summer monsoon during June to September is the most dominant annual climate feature over the south Asia region,

✉ C. K. Unnikrishnan
unnikrishnack@gmail.com

M. Rajeevan
rajeevan@tropmet.res.in

[1] National Centre for Medium Range Weather Forecasting, ESSO MoES, Sector-62, Noida, India

[2] Indian Institute of Tropical Meteorology, Pune 411 008, India

[3] Sri Venkateswara University, Tirupati 517 502, India

and it exhibits variability in all time scales from diurnal to multi-decadal. Prediction of interannual variability of monsoon is important due to its direct impact on agriculture, water resources, and economy over the region. The anomalous slowly varying boundary conditions form the basic premises of seasonal prediction (Charney and Shukla 1981; Shukla 1981). South Asian monsoon variability is mainly influenced by the boundary forcing from both the tropical oceans and land. The role of tropical oceans, especially the equatorial Pacific Ocean on influencing the South Asian monsoon rainfall, is well documented (Sikka 1980; Rasmusson and Carpenter 1983; Webster and Yang 1992; Gadgil et al. 2007). However, the role of land surface processes on the monsoon variability is not well understood.

Land surface acts as the lower boundary for the atmosphere, and it regulates the energy partition and water balance and influences the regional climate. In this context, soil moisture plays a major role in the interaction between the land surface and the atmosphere. Soil moisture influences surface energy balance components through its effects on evapotranspiration or latent heat flux (Zhang et al. 2011). Anomalies in surface fluxes induced by soil moisture may cause precipitation anomalies over some regions (Delworth and Manabe 1989). The global coupling of land surface and atmosphere shows a wide spectrum of spatial and temporal variations. The global scale coupling of soil moisture and precipitation was investigated by Koster et al. (2004, 2006). They identified the global coupling hotspots, where the soil moisture interaction directly influences summer precipitation variability. The Indian summer monsoon region was also identified as one of the hot spots of the land surface coupling. The land surface coupling is found to be strong over the transition zones between wet and dry climate regimes.

Quality-controlled soil moisture observations are generally scarce over the south Asian region. Therefore, atmospheric general circulation models (AGCMs) helped us to have our

current understanding of land-atmosphere coupling. In the early 1980s, Shukla and Mintz (1982) and Yeh et al. (1984) made pioneering studies and suggested strong sensitivity of the climate response with respect to soil moisture anomalies. The analyses of Seneviratne et al. (2006) showed that land surface coupling is significantly affected by global warming and acts as a major player for climate change based on the simulation of regional climate model (RCM) and general circulation model (GCM) experiments. Zhang et al. (2008) studied the influence of land surface processes in the interannual scale over the contiguous USA. There are many other studies which showed the importance of land surface processes in the prediction of precipitation using atmospheric models (van den Hurk et al. 2012; Koster et al. 2004, 2006, 2010 and 2011; Guo et al. 2011 and 2012; Fennessy and Shukla 1999). Steiner et al. (2009) showed that land surface coupling can influence the regional circulation and precipitation over the regions exhibiting strong hydroclimatic gradients. However, the impacts of regional land surface coupling on south Asian monsoon interannual variability are not very well understood.

There are some studies on the role of land surface processes and especially soil moisture on the Asian monsoon variability (Shukla and Mintz 1982; Webster 1983; Meehl 1994; Ferranti et al. 1999; Kim and Hong 2007; Takata et al. 2009). Douville et al. (2001) studied the role of soil moisture on the Asian and African monsoon systems and found different sensitivity for the Asian and African monsoons to the land surface hydrology. It is seen that the African monsoon is more influenced by the soil moisture feedbacks. Later, the study by Douville (2002) emphasized the relevance of soil moisture for seasonal climate predictions. Observational and modeling studies over the African monsoon region have shown the importance of antecedent rainfall patterns affects new storms in the region (Taylor et al. 2011). Bellon (2010) studied how land-atmosphere interaction influences the northward-propagating intraseasonal oscillation in the Asian monsoon region. Zhang et al. (2011) studied the land surface coupling over the East Asian monsoon region, which suggested that soil moisture makes a dominant contribution to rainfall variability over the climatic and ecological transition zones of the East Asian monsoon region. Saha et al. (2011) proposed the importance of land surface process in pre-onset monsoon season and showed that dry (wet) pre-onset land surface condition increases (decreases) the Indian seasonal monsoon rainfall. Further, Saha et al. (2012) proposed a large-scale nature of soil moisture, intraseasonal oscillation feedback, which alters lower level atmospheric conditions. Modeling of soil moisture is essential for reliable simulation and forecasting of the Indian summer monsoon (Asharaf et al. 2012) as they showed that pre-monsoon soil moisture has a significant influence on the Indian monsoon rainfall. Sijikumar et al. (2013) showed the sensitivity of model land surface orography on the south Asian monsoon rainfall in the Weather Research and

Forecasting (WRF) regional climate model. They showed that the model orography can significantly impact the model rainfall and wind over the monsoon region.

Large uncertainties exist in AGCM studies of land-atmosphere interactions especially on local to regional scales (Dirmeyer et al. 2006). The Global Land-Atmosphere Coupling Experiment (GLACE-1) demonstrated a large spread in land-atmosphere coupling hot spots among many AGCMs (Koster et al. 2004, 2006; Guo et al. 2006). The studies showed that the models have large systematic errors compared to observed relationships between land and the atmosphere on the local and regional scales. However, compared to AGCMs, regional climate models (RCMS) are more skillful in simulating regional climate characteristics. RCM assessment of soil moisture influences on interannual climate variability is receiving more attention recently. The impact of land-atmosphere coupling in influencing interannual summer climate variability over the contiguous USA (Zhang et al. 2008) and over East Asia (Zhang et al. 2011) was investigated by using the WRF RCM. They found that land surface plays a critical role in influencing summer climate variability over the climatic and ecological transition zones.

In this paper, we address the role of land surface coupling on the Indian monsoon variability using a regional climate model during the recent decade. The main objective of the present study is to improve our understanding of the role of land-atmosphere coupling on the interannual variability of the Indian monsoon climate with a WRF regional climate model. This study also evaluates coupling of surface fluxes (latent heat and sensible heat) and boundary layer height over the monsoon region, which was not studied previously. In Section 2, the regional model configuration, the model experimental set up, and the methodology of calculation of land surface coupling parameters are explained. Sections 3 discusses about the model performance and validation of model climatology. Sections 4, 5, and 6 discuss the coupling of soil moisture with air temperature and rainfall over the south Asian region. In Section 7, the results are summarized.

2 Model configuration and experimental setup

For the present study, the WRF ARW version 3.3 was used as the regional climate model to simulate the land surface coupling over the south Asian monsoon region. The WRF ARW model is a fully compressible non-hydrostatic and Eulerian model. It uses the terrain following hydrostatic pressure coordinate and the Arakawa–C grid. The model equations conserve the scalar variables. In this configuration, the third-order Runge-Kutta scheme was used for integration and employed fifth-order advection schemes. WRF high-resolution regional climate model was used for the simulation of the climatology of monsoon precipitation in previous

studies (Mukhopadhyay et al. 2010; Srinivas et al. 2013). The WRF regional climate model configuration used in this study is similar to that of previous experiments made by Bhate et al. (2012) over the Indian monsoon region.

The model was implemented with a horizontal resolution of 45 km, 28 pressure levels with model top pressure at 10 hPa. The model domain covers the Indian summer monsoon region (40 E–120 E and 10 S–40 N) (Fig. 1). The initial conditions and boundary conditions for the model simulations were derived from the final analysis (FNL) data of 1° × 1° horizontal resolution from the National Centers of Environmental Prediction (NCEP). The lateral boundary conditions were updated every 6 h. The FNL sea surface temperature (SST) data were used as the lower boundary conditions. The model was initialized from 1st May 2000 and 12-year integrations were made up to December 2011.

The WRF model was configured with the following physical parameterization schemes: the microphysics scheme of Lin et al. (1983), Monin-Obukhov similarity scheme (Monin and Obukhov 1954) for surface layer, Yonsei University scheme for planetary boundary layer (PBL) (Hong and Dudhia 2003), Dudhia scheme (Dudhia 1989) for short wave, and RRTM scheme for long wave (Mlawer et al. 1997). The unified Noah land surface model (Chen and Dudhia 2001) was used as the land surface model, which consists of four soil layers with the thicknesses of 10, 30, 60, and 100 cm from the top to the bottom and one canopy layer. It uses the Reynolds number-based approach for the estimation of the ratio between the roughness lengths for heat and momentum transfer. For the convective parameterization, Betts Miller Janjic scheme (Betts 1986; Betts and Miller 1986; Janjic

1994) was used. Figure 1 shows the topographic heights used in the model analysis domain.

Two long-term simulations were performed similar to the studies of Koster et al. (2004), Seneviratne et al. (2006), and Zhang et al. (2008, 2011). In the control experiment (CTL), the model was integrated from the year 2000 to 2011 and allowed the soil moisture interaction with the atmosphere using a coupled land surface model. In the second experiment (CSM), the soil moisture evolution at each time step was replaced with the climatology of soil moisture taken from the control run. Thus, the CSM experiment removes the interannual variability of soil moisture which exists in the first CTL experiment. This will allow us to assess the role of interactive soil moisture in influencing the climate variability of the south Asian summer monsoon. In CTL experiment, the model integration started from 1st May 2000 and integrated up to 30th September 2011. For the CSM experiment, the model was integrated from 1st June up to 30th September for every year separately during 2000 to 2011. The results of the first 13 months, from 1 May 2000 to 31 May 2001, were removed from the analysis to account for the model spin up to minimize the initialization effects of soil moisture and soil temperature. The model performance in simulating the mean summer monsoon was evaluated by analyzing the CTL experiment for the period 2000–2011. The model-simulated rainfall, 850 hPa wind, and surface 2 m temperature were compared with the observations. The tropical rainfall measuring mission (TRMM) product (Huffman et al. 2007) 3B42 was used to compare the model-simulated rainfall over the analysis domain. The TRMM rainfall is re-gridded to 0.5 degree for the comparison of the model results. ECMWF ERA-Interim reanalysis

Fig. 1 Terrain height (km) over the WRF model domain used in the study
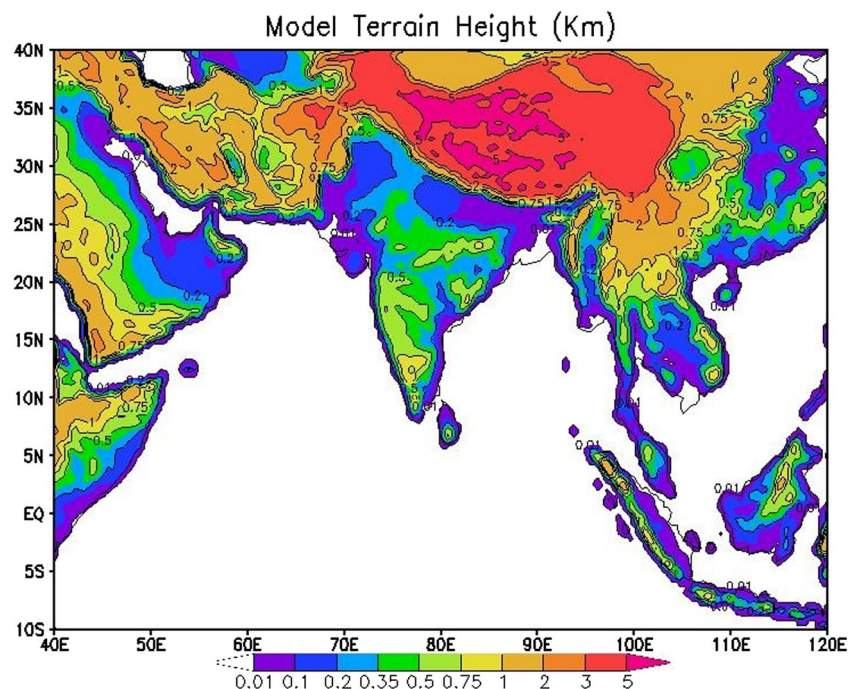
wind at 850 hPa was used to compare the simulated wind at 850 hPa. For the evaluation of 2 m air temperature, the observations from the Climate Prediction Center (CPC), NCEP (Fan and van den Dool 2008) were used. This data set is a global land monthly data set at a resolution of 0.5°. This temperature data set was developed using station observations from the Global Historical Climatology Network (GHCN) and Climate Anomaly Monitoring System (CAMS). The details of model evaluation are discussed in Section 3 of the paper. The soil moisture observations from satellite are used for soil moisture comparison. European Space Agency (ESA) is providing the gridded active and passive soil moisture from satellites (Wagner et al. (2012)). This data is available from the following web address: http://www.esa-soilmoisture-cci.org/. The soil texture data used in WRF model is based on a hybrid 30-s State Soil Geographic Database (STATSGO) and 5-min Food and Agriculture Organization (outside US), and it also used 16 category soil texture (Miller and White 1998). The soil types used in the model domain is shown in Fig. 2.

To investigate the coupling between soil moisture and the atmosphere over the monsoon region, we calculated the difference in the standard deviation of rainfall and temperature between the CTL and CSM experiments, applied variance analysis, and calculated a revised coupling strength parameter similar to Zhang et al. (2008 and 2011). The CTL and CSM experiments allow us to separate the contribution of interaction of soil moisture in the interannual variability of rainfall and temperature. The difference between standard deviation (σ) of CTL and CSM is given by Eq. (1).

$$d\sigma_x = \sigma_x(\text{CTL}) - \sigma_x(\text{CSM}) \qquad (1)$$

where x is mean June to September daily rainfall and 2 m air temperature. This difference allows us to assess the contribution of interactive soil moisture in the interannual variability of rainfall and temperature. The $d\sigma_x$ shows the sensitivity of land-atmosphere coupling on summer climate variability and depends on the variable (x). This mainly depends on the location, and it shows the direct impact of the land surface coupling on the variability of variable (x).

Percentage of variance (PV) of rainfall and temperature was calculated by applying the variance analysis. The advantage of PV is that it does not depend on the location. It is a measure of the relative contribution of land-atmosphere coupling to interannual rainfall and temperature variability over the monsoon region. Percentage of variance during the period, June to September, is estimated using the following Eq. 2.

$$\text{PV}_x = \frac{\sigma_x^2(\text{CTL}) - \sigma_x^2(\text{CSM})}{\sigma_x^2(\text{CTL})} \qquad (2)$$

where x is rainfall or 2 m air temperature. σ_x^2 is the monthly mean variance of variable x. This percentage of variance change calculated is related to the coupling of land surface processes to the variable x, i.e., it is the percentage fraction of the variance of a specific variable in CTL experiment due to the soil moisture interactions. It is a measure of the relative contribution of interactive soil moisture to interannual variability of variable (x). Further, the coupling strength parameter was used to investigate the role of soil moisture coupling in previous studies (Koster et al. 2000; Seneviratne et al. 2006). This paper uses the revised GLACE-1 coupling strength parameter similar the one used by Zhang et al. (2008 and 2011).

Fig. 2 The soil types used in the model domain (data source SATASGO)
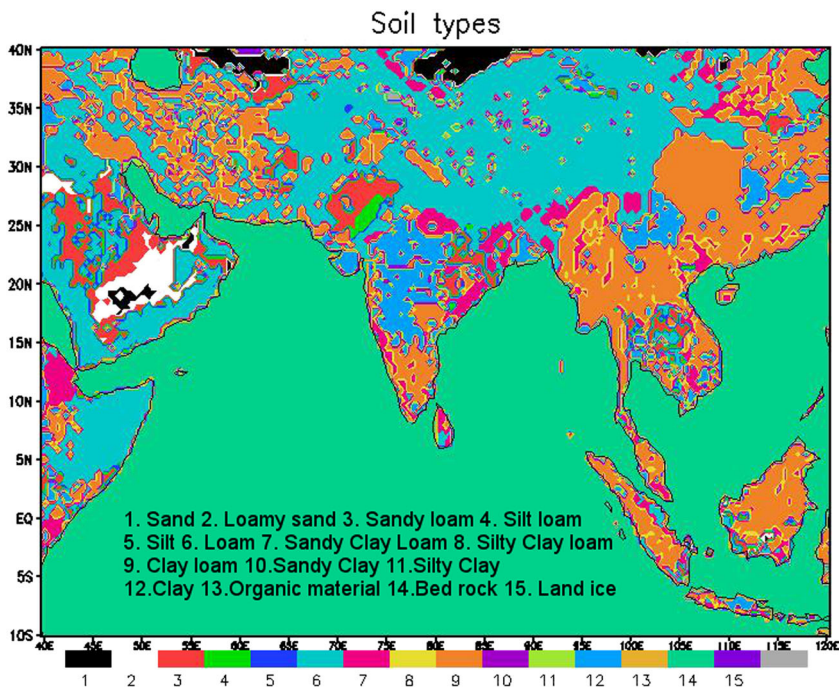
For rainfall and temperature, 120 days of simulations were aggregated into 24 pentads (5-day means). For each pentad, we have 10 years of model simulations.

The difference in the pentad group values are related to the interannual variations of the variable (x). The time series similarity of a variable x (Ω_x) is calculated using Eq. (3)

$$\Omega_x = \frac{24\sigma_{x1}^2 - \sigma_x^2}{23\sigma_x^2} \tag{3}$$

where σ_{x1}^2 is the variance of the 24 group average time series for the 10 years in the time series. σ_x^2 is the variance of pentad mean climate variable computed from all the pentad (24×10) values. The coupling strength parameter for the variable (x) is calculated using Eq. (4).

$$\Delta\Omega_x = \Omega_x(\text{CTL}) - \Omega_x(\text{CSM}) \tag{4}$$

where Ω_x (CTL) accounts for the interannual variability of a variable (x) induced by all factors. But Ω_x(CSM) include the effect of climatological soil moisture. Coupling strength of the variable (x) is calculated as the difference ($\Delta\Omega_x$) (Eq. (4)). Coupling strength parameter is a measure of the soil moisture interaction-induced similarity of the interannual variations between pentads of variable (x).

The coupling strength calculated using the model simulations depends on the performance of the RCM and various other factors including the parameterization schemes used in the configuration of the model. Model-simulated rainfall depends on many factors including the convective parameterization scheme considered in the model (Srinivas et al. 2013). It also depends on the feedback and internal dynamics of the model. Model horizontal resolution, orography, heat exchange coefficients for heat and moisture, use of climatological vegetation fraction, vegetation type-induced biases, etc. have an impact in the coupling strength. Compared to global models, regional climate models have the advantage of estimation of land-atmosphere coupling due to high spatial resolution and better land surface parameterizations.

3 Simulated model climatology

In this section, the model-simulated (CTL) rainfall and temperature at 2 m are evaluated with the observed data sets. TRMM 3B42 data gives the rainfall over both land and ocean regions. Joshi et al. (2012) show that TRMM 3B42 rainfall estimate is comparable over the Indian monsoon region during the seasonal time scale. The model mean and standard deviation of rainfall are compared with the observations. For this purpose, the TRMM daily data is averaged to 0.5° over the model domain. Figure 3 shows the comparison of TRMM and model mean rainfall

patterns. The model is able to simulate the mean features of the monsoon rainfall over south Asia reasonably well. However, there are biases. There is a large positive bias over the Bay of Bengal and central parts of India. The model simulates maximum rainfall along the west coast of India and northeast India. Similarly, the model captures minimum rainfall over northwest India and southeast peninsular India. In the model, the monsoon trough is located slightly south of its normal position and the east central rainfall maximum is shifted southwards. In Fig. 4, the standard deviation of rainfall is compared with the observations. In general, the model exhibits a larger standard deviation of monsoon rainfall compared to the observations. The result shows that the interannual variability are higher over the west coast region, northeast India, central India, and foot hills of the Himalayas in the model.

The ECMWF ERA-Interim reanalysis wind at 850 hPa was used to compare the simulated model wind as shown in Fig. 5. The comparison shows that the model simulates a much stronger lower tropospheric monsoon flow. The low level westerly jet stream is much stronger in the model compared to the reanalysis data. Over the Bay of Bengal, the model simulates a large horizontal wind shear, which may be responsible for the excessive rainfall over the Bay of Bengal (Bhate et al. 2012).

The satellite-observed soil moisture is used to compare the mean model soil moisture during the JJAS period. Figure 6 shows the comparison of volumetric soil moisture. The model surface soil moisture (0–10 cm) is compared to the ESA's gridded active and passive surface soil moisture. However, the satellite soil moisture represents only the first few centimeters of the soil surface, and satellite-based soil moisture products are also sensitive to the surface roughness and vegetation. In Fig. 6, the soil moisture values over land below 0.05 are masked with white color. It is observed that model soil moisture is overestimated compared to the observations. The soil moisture index (Betts 2004) is an additional measure of soil moisture content that incorporates the information about the field capacity and wilting point. Soil moisture index (SMI) shows the amount of free soil moisture available for evapotranspiration. The SMI from the model and ESA satellite observations are also compared (Fig. 7). In Fig. 7, the values between 0 and 1 are shaded with different colors; other values are masked with white. The model shows a higher SMI compared to the observation. The difference in soil moisture between the model and observation suggests that the estimated land surface coupling can have a bias compared to the actual land surface coupling. For the evaluation of 2 m temperature of the model simulations, the station-based GHCN-CAMS temperature data from Climate Prediction Center (CPC), NCEP was used. Figure 8 shows the comparison of mean temperature pattern of observation and the model simulations. The model simulates the spatial pattern of mean

Fig. 3 Seasonal monsoon rainfall
(June to September—2001–
2011): **a** TRMM and **b** model
simulation (mm/day)

Fig. 3 Seasonal monsoon rainfall (June to September—2001–2011): **a** TRMM and **b** model simulation (mm/day)
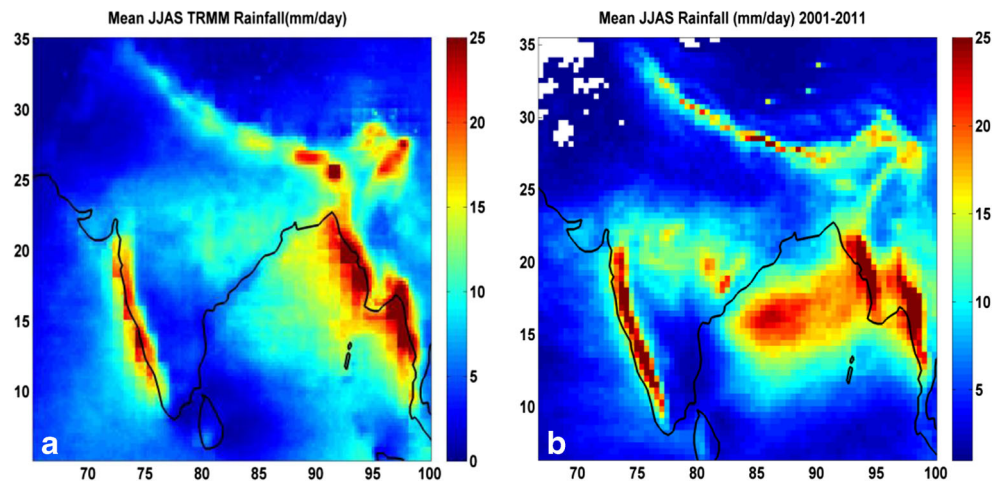
temperature over south Asia reasonably well. However, the model has shown a cold bias over the western hilly regions, where the model underestimates mean temperature. Over north and northwest India, where the model has a dry bias in rainfall, the model simulates a warmer temperature compared to observations. Comparison of the standard deviation of mean temperature is shown in Fig. 9. The temperature variability is maximum over northwest India and central India. The model overestimates the standard deviation of mean temperature over northwest India and the Tibetan plateau region. The uncertainties in model-simulated cloud cover, radiation, and precipitation have caused this difference. In the next section, we discuss the coupling of soil moisture with surface air temperature.

4 Coupling of soil moisture and surface air temperature

In this section, the role of soil moisture on the temperature variability is examined using the model experiment results. For this purpose, the difference between standard deviation

of temperature ($d\sigma_x$) is calculated using Eq. (1) by using the CTL and CSM experiments. Further, percentage of variance and modified coupling strength over the region were also calculated. In addition to mean daily temperature (T_{mean}), maximum daily temperature (T_{max}) and minimum daily temperature (T_{min}) were also considered. Figure 10 shows the difference of standard deviation of T_{mean}, T_{max}, and T_{min} between the CTL and CSM experiments. The differences which are statistically significant at 95 % level are shown as dots.

The difference in standard deviation of T_{mean} is maximum over northwest India, central India, and southeast peninsula. The difference in standard deviation of T_{max} and T_{min} is also showing the similar pattern but with smaller amplitudes. In comparison, the difference of standard deviation in maximum temperature has shown higher values, compared to minimum temperature. This may be due to the fact that maximum temperature depends on the net radiation at the surface and partitioning of latent heat flux and sensible heat flux and mainly controlled by the soil moisture availability. The minimum temperature occurs during the night time, and it is mainly controlled by the large-scale circulation over the region and radiative fluxes.

Fig. 4 Standard deviation seasonal monsoon rainfall (June to September): **a** TRMM and **b** model simulation (mm/day)
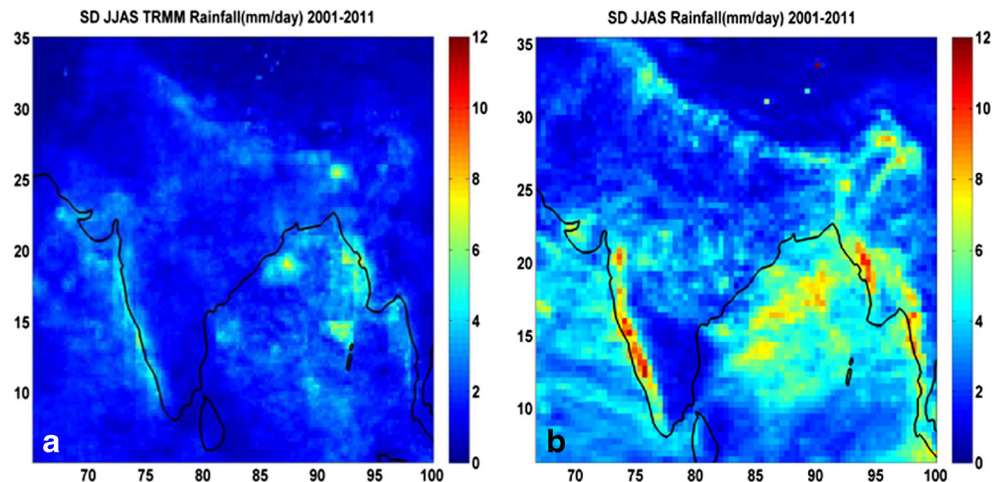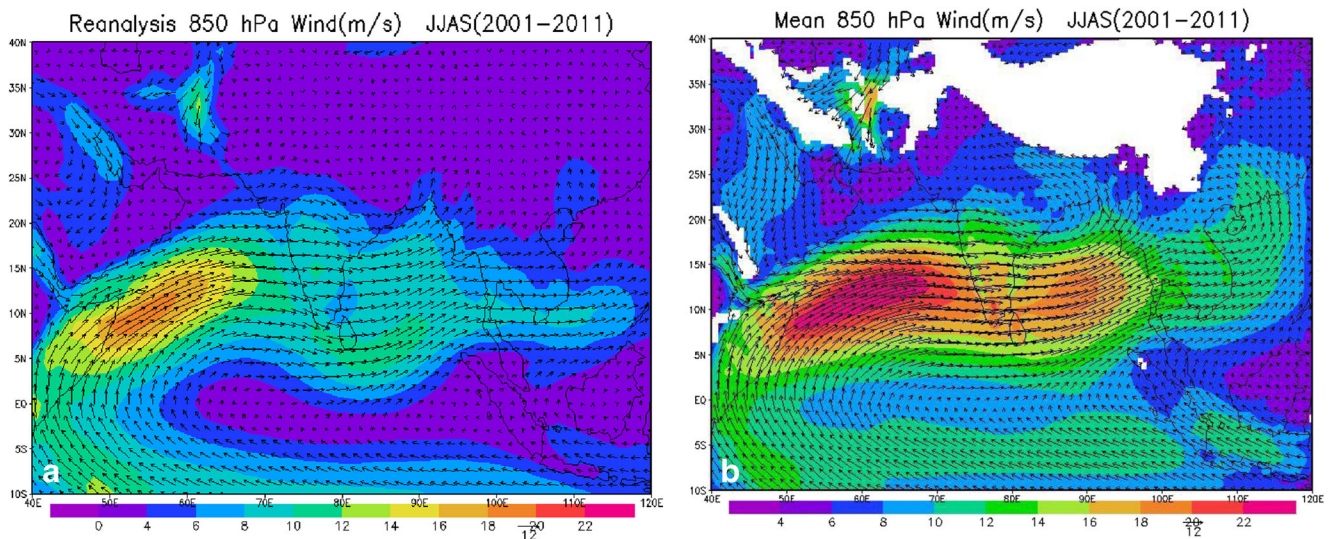
Fig. 5 Seasonal mean (June to September) 850 hPa wind: **a** ECMWF ERA-Interim reanalysis and **b** model simulation (m/s)

The percentage of variance of temperature due to interactive soil moisture is calculated using the Eq. (2). The percentage of variance of temperature for T_{mean}, T_{max}, and T_{min} is shown in Fig. 11a, c, e). Maximum percentage variance of temperature is observed over the arid and semi-arid regions over India. The percentage of variance of T_{mean} is the highest over northwest India, parts of central India and southeast India, Bangladesh, and the foothills of the Himalayas where more than 30 % variance is explained. The T_{max} and T_{min} also show similar spatial patterns. However, the magnitude of variance change is much higher for maximum temperature compared to minimum temperature. Thus, it can be inferred that maximum temperature is much more influenced by soil moisture variations compared to minimum temperature.

The coupling strength parameter is also calculated using Eq. (4). The spatial pattern of coupling strength calculated for the period 2001–2011 is shown in Fig. 11b, d, f. Coupling strength is more over northwest India and western parts of central India. The foothills of the Himalayas show a large coupling parameter for temperature. However, east central parts of India show weaker coupling strength. This result is comparable with the previous study of Koster et al. (2006) over the region and in which spatial pattern of coupling is found to be smoother. These results provide a better regional coupling scenario. The results show better coupling over southeast India and less coupling over heavy rainfall areas like west coast and monsoon trough region.

Fig. 6 The observed surface soil moisture (m³/m³) from ESA (*left*) and model soil moisture (0–10 cm) (*right*) during the monsoon season
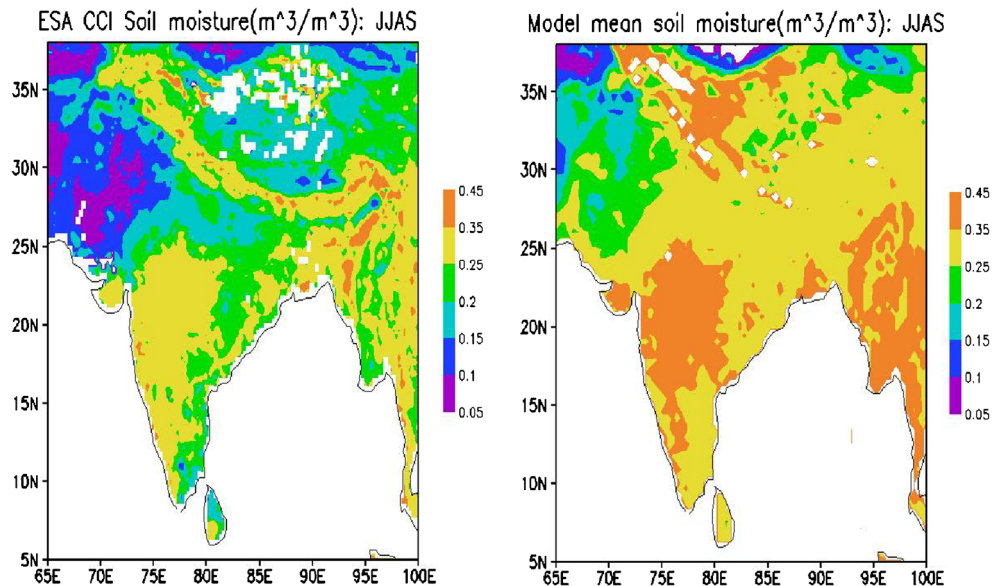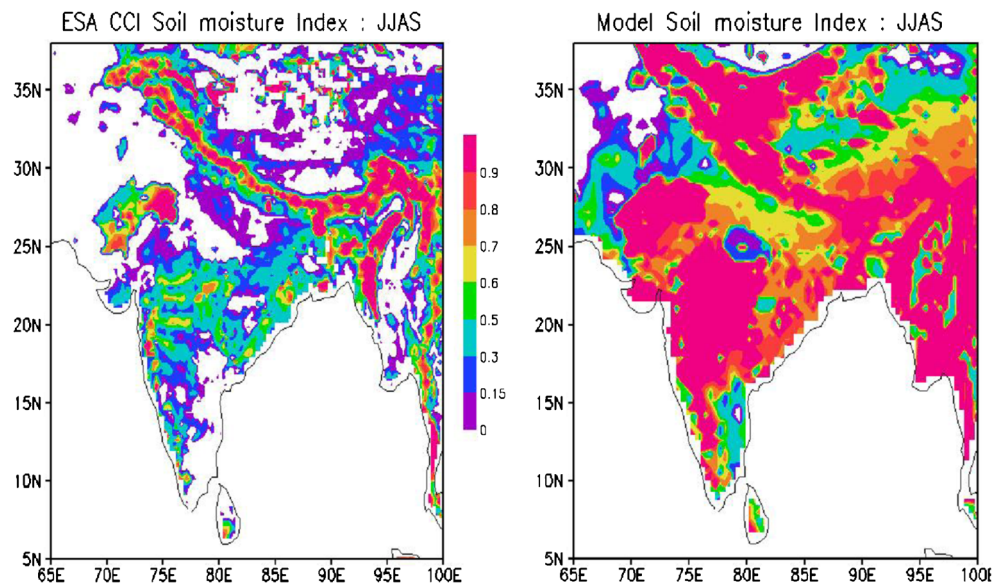
Fig. 7 The observed surface soil
moisture index from ESA (*left*)
and model soil moisture index (0–
10 cm) (*right*) during the
monsoon season

5 Coupling of soil moisture and rainfall

In this section, we examine the effect of soil moisture coupling on rainfall simulations over the south Asian monsoon region. Figure 11 shows the standard deviation of rainfall between CTL and CSM. The differences which are statistically significant at 95 % level are shown as dots. The differences in the standard deviation of rainfall between CTL and CSM are calculated separately for total rainfall, large-scale rainfall, and cumulus rainfall, and the results are shown in Fig. 12a–c, respectively. For total and large-scale rainfall, the maximum soil moisture influence is seen over northwest India and central India, i.e., over the seasonal monsoon trough region. Influence of soil moisture coupling is not observed elsewhere in the south Asian monsoon region. For the cumulus rainfall/convective rainfall also, maximum coupling is seen over northwest region and the monsoon trough region especially the region where the monsoon synoptic systems like monsoon

lows and depressions are more active. This suggests the need for more observational and modeling studies on the soil moisture interactions in the synoptic-scale processes in the monsoon trough region during the summer monsoon season. In the convective rain case, the difference between CTL and CSM results is slightly smaller compared to large-scale rainfall.

Further, the variance analysis is applied and the percentage of variance of rainfall due to the soil moisture interaction is calculated using Eq. (2). Similarly, the coupling strength parameter is also calculated using Eqs. (3) and (4). The percentage of variance of rainfall and estimated coupling strength parameter are shown in Fig. 11. Percentage of variance and coupling strength parameters remove the spatial weight of the amount of rainfall over the domain during the season. These two parameters are calculated for total rain, large-scale rain, and convective rain separately. Figure 13a, c, e shows percentage of variance, and Fig. 13b, d, f shows coupling strength parameters for the total rain, large-scale rain, and cumulus rain.

Fig. 8 Seasonal (June to
September) mean 2 m
temperature (degree): **a**
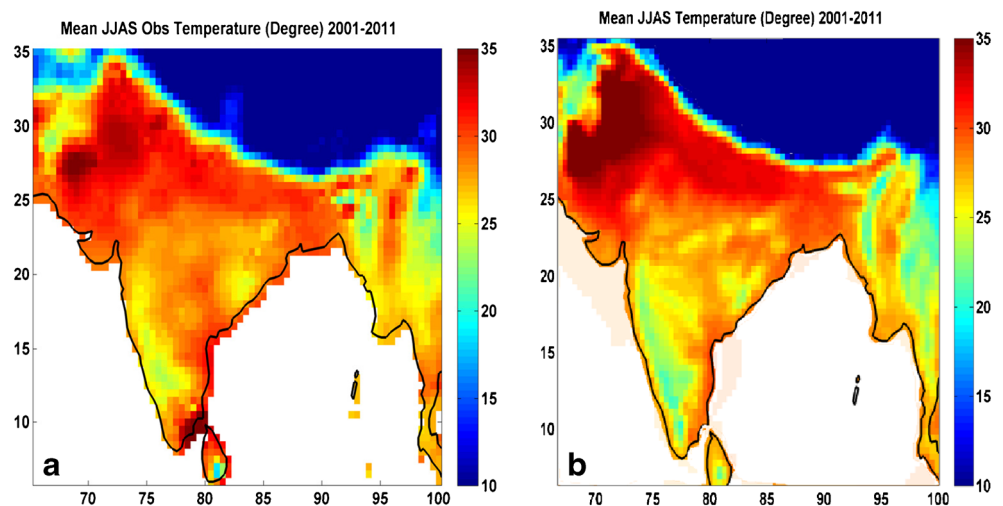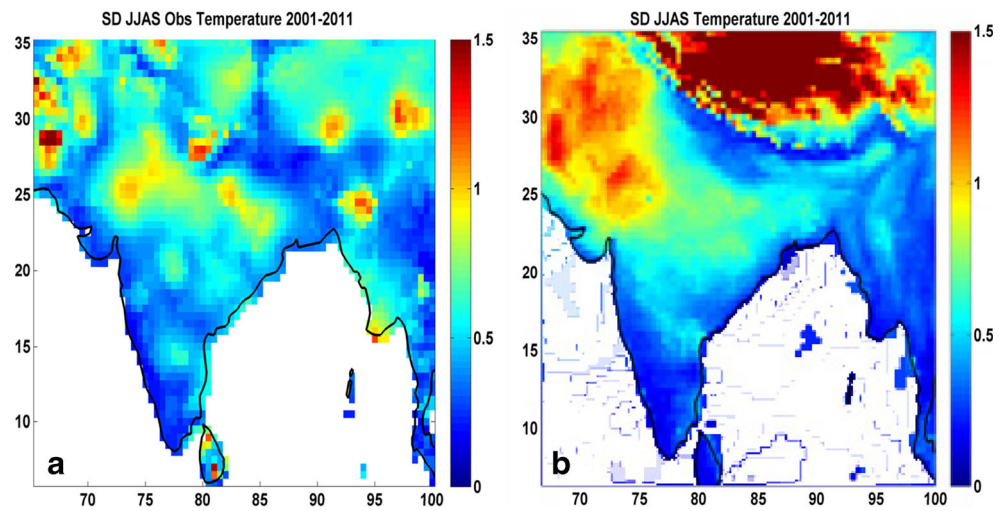observation and **b** model
simulation

Fig. 9 Standard deviation of seasonal (June to September) 2 m temperature: **a** observation and **b** model simulation

The percentage of variance of total rainfall shows a similar pattern and matches with the difference between the standard deviation of CTL and CSM shown in Fig. 12a. Maximum coupling due to soil moisture is seen over northwest and central India. The coupling strength parameters give a fine structure of the coupling between the land surface and atmosphere.

Stronger coupling parameter is seen over central India and the monsoon trough region. The scattering of coupling regions also shows importance of land cover on regional land surface coupling. The large-scale rainfall is also showing the similar pattern of land surface coupling that of the total rainfall. Figure 13c, d shows the percentage of variance and coupling
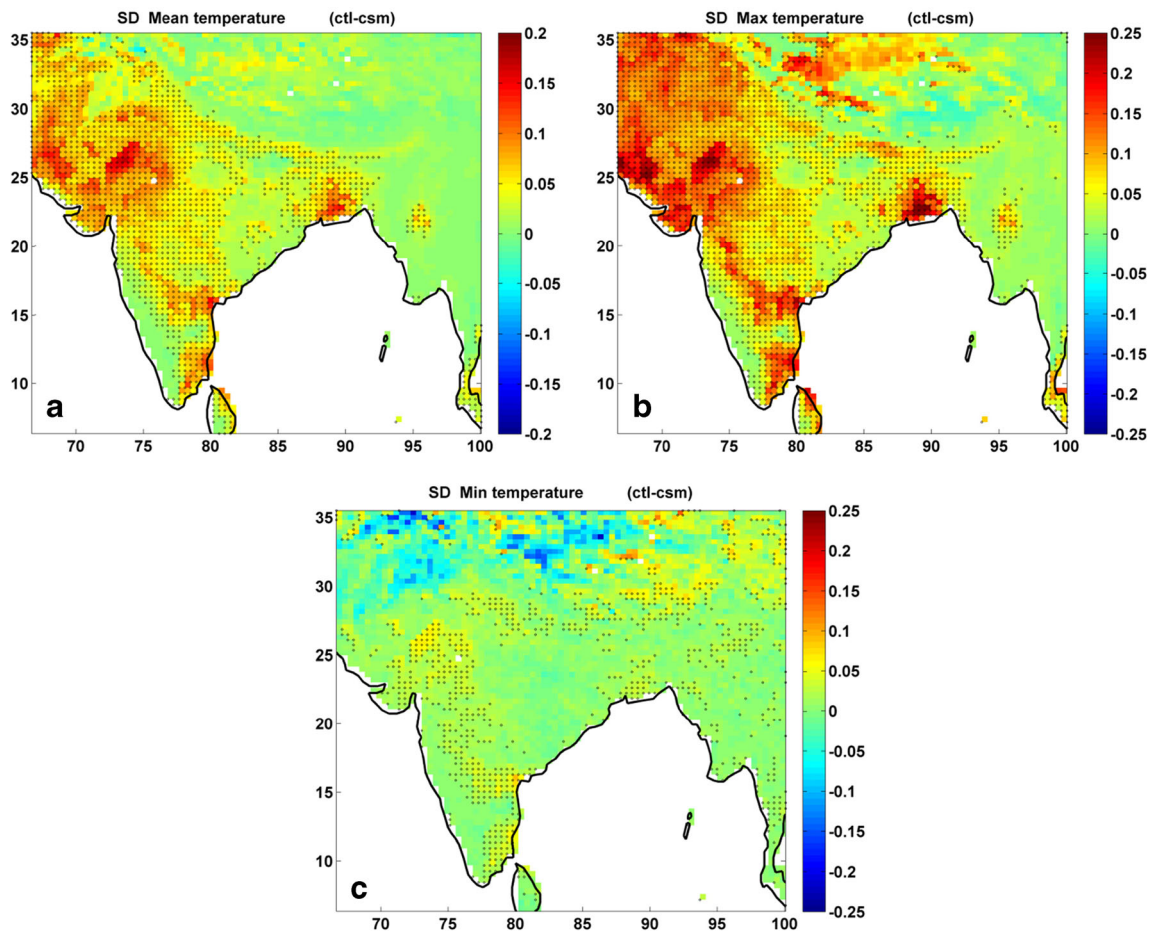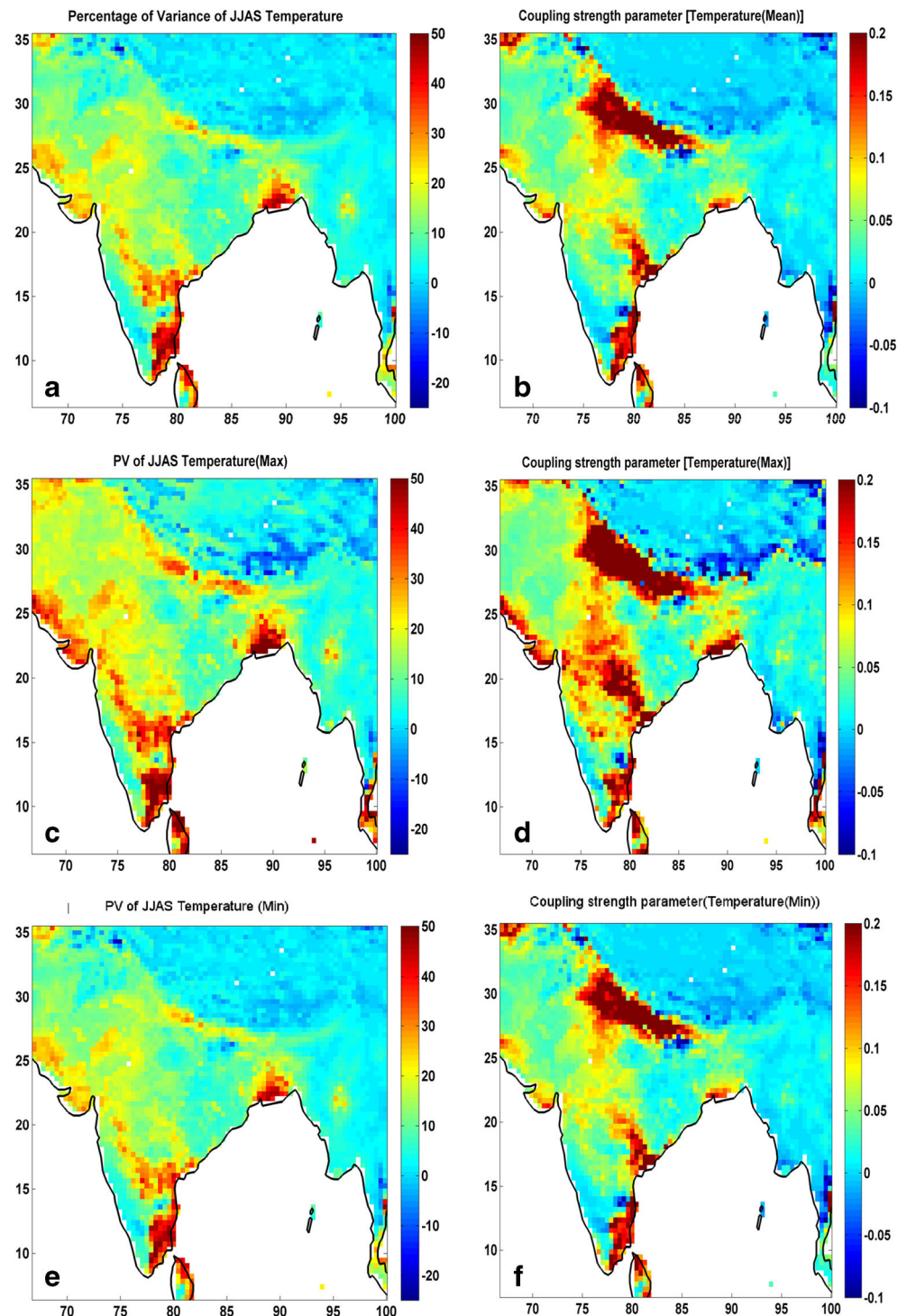

Fig. 10 The difference between the standard deviations of CTL- and CSM-simulated 2 m temperature: **a** mean, **b** maximum, and **c** minimum (areas significant at 0.05 levels are marked with *dots*)

Fig. 11 The PV and coupling strength parameters for **a, b** T_{mean}, **c, d** T_{max}, and **e, f** T_{min}, respectively

strength parameters for the large-scale rain. Maximum values of percentage of variance and coupling parameter are observed over the central India and the monsoon trough region. This result shows the strong interaction of the synoptic systems and land surface processes over the monsoon trough region. Similarly, Chang et al. (2009) also showed that if the surface receives heavier rainfall a week ahead of the synoptic system, then the intensity of the system

is maintaining for a longer period. The remaining area of the study does not show any strong coupling to the land surface. Figure 13e, f shows the percentage of variance and coupling strength parameters for the cumulus rain. For cumulus rainfall, maximum percentage of variance due to the soil moisture interaction is seen over northwest India and neighborhood. A maxima is seen over the monsoon trough region, where the synoptic systems like monsoon trough and monsoon lows
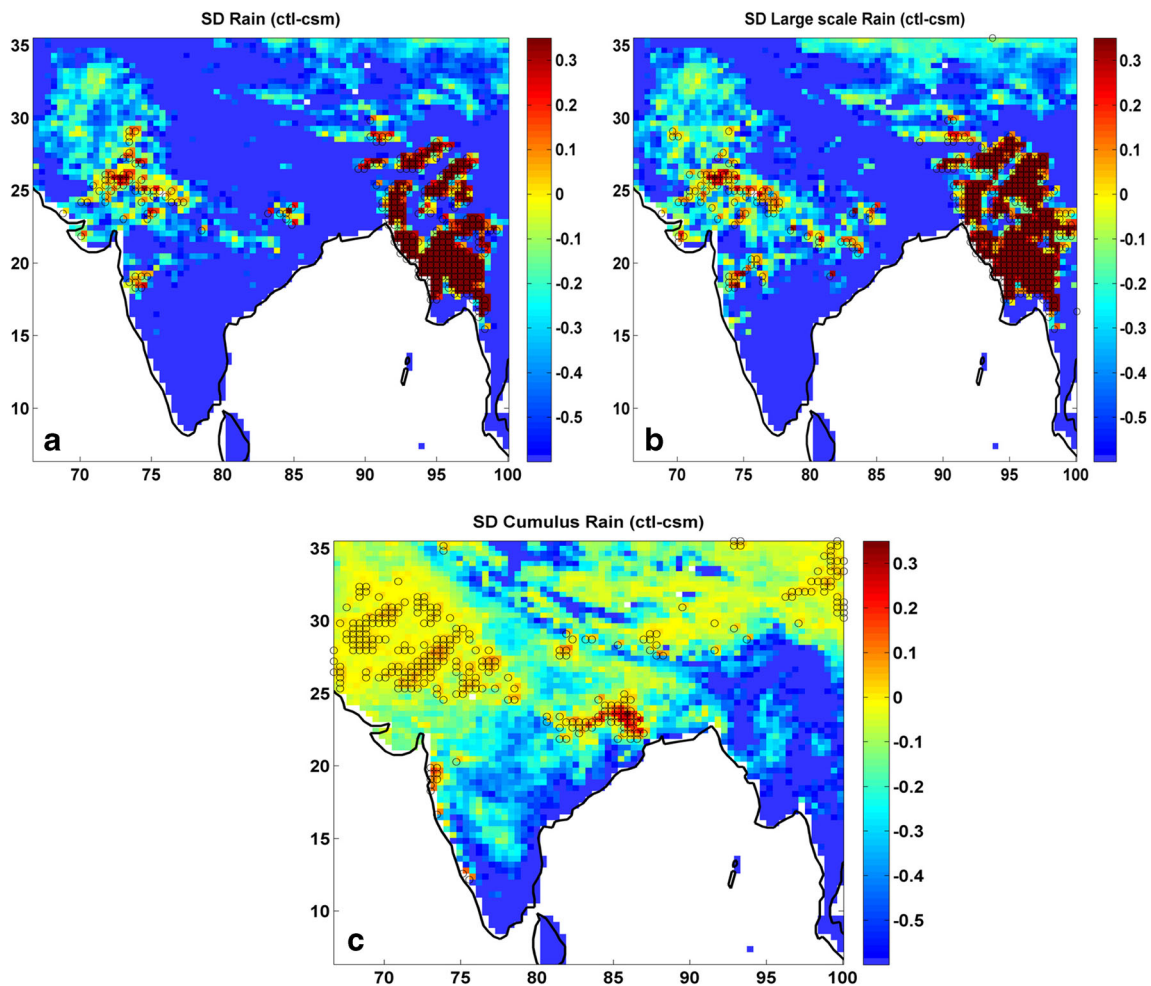
Fig. 12 The difference between the standard deviations of CTL and CSM rainfall: **a** mean, **b** maximum, and **c** minimum, respectively (areas significant at 0.05 levels are marked with *dots*)

play a dominant role. The coupling strength parameter calculated for cumulus rainfall does not show significant spatial features. This may be due to the comparatively lower values of convective rainfall amount compared to the large-scale rainfall. But it is clear from the percentage of variance analysis that the cumulus rainfall variability is coupled to land surface processes over the monsoon trough region where synoptic-scale interaction is more active. It is also noticed that some of the west coast belts (like Maharashtra, Kerala) show a coupling of the cumulus rain and soil moisture. Results show that the large-scale rain is more coupled to land surface compared to the convective rainfall over the monsoon region. However, over Southeast Asia, the land surface is more coupled to convective rainfall than the large-scale rainfall (Zhang et al. 2011). This shows that the land surface is coupled to both monsoon regions differently.

Our analysis of difference of the standard deviation of rainfall between CTL and CSM, variance analysis, and coupling strength parameter showed that the monsoon trough region and northwest India rainfall is coupled strongly to land

surface process, through soil moisture. The interaction of soil moisture and rainfall is dominant over these regions. This result shows the strong coupling of synoptic systems over the monsoon trough regions which propagate from Bay of Bengal to central India. This result is comparable with the previous coupling results of Koster et al. (2006) done for USA and China. However, we find a finer scale structure of regional coupling over the region in the recent decade. Further, the coupling of soil moisture to surface heat fluxes like sensible heat flux, latent heat flux, and PBL height is evaluated and discussed in the next section.

6 Coupling with surface fluxes

In this section, we investigate the coupling process related to the observed coupling spots over the monsoon region. Soil moisture is directly coupled to the atmosphere through the surface fluxes. To investigate the role of soil moisture and sensible heat flux, we calculated the product of difference

Fig. 13 The PV and coupling
strength parameters for rainfall **a**,
b total rain, **c**, **d** large-scale rain,
and **e**, **f** cumulus rain, respectively
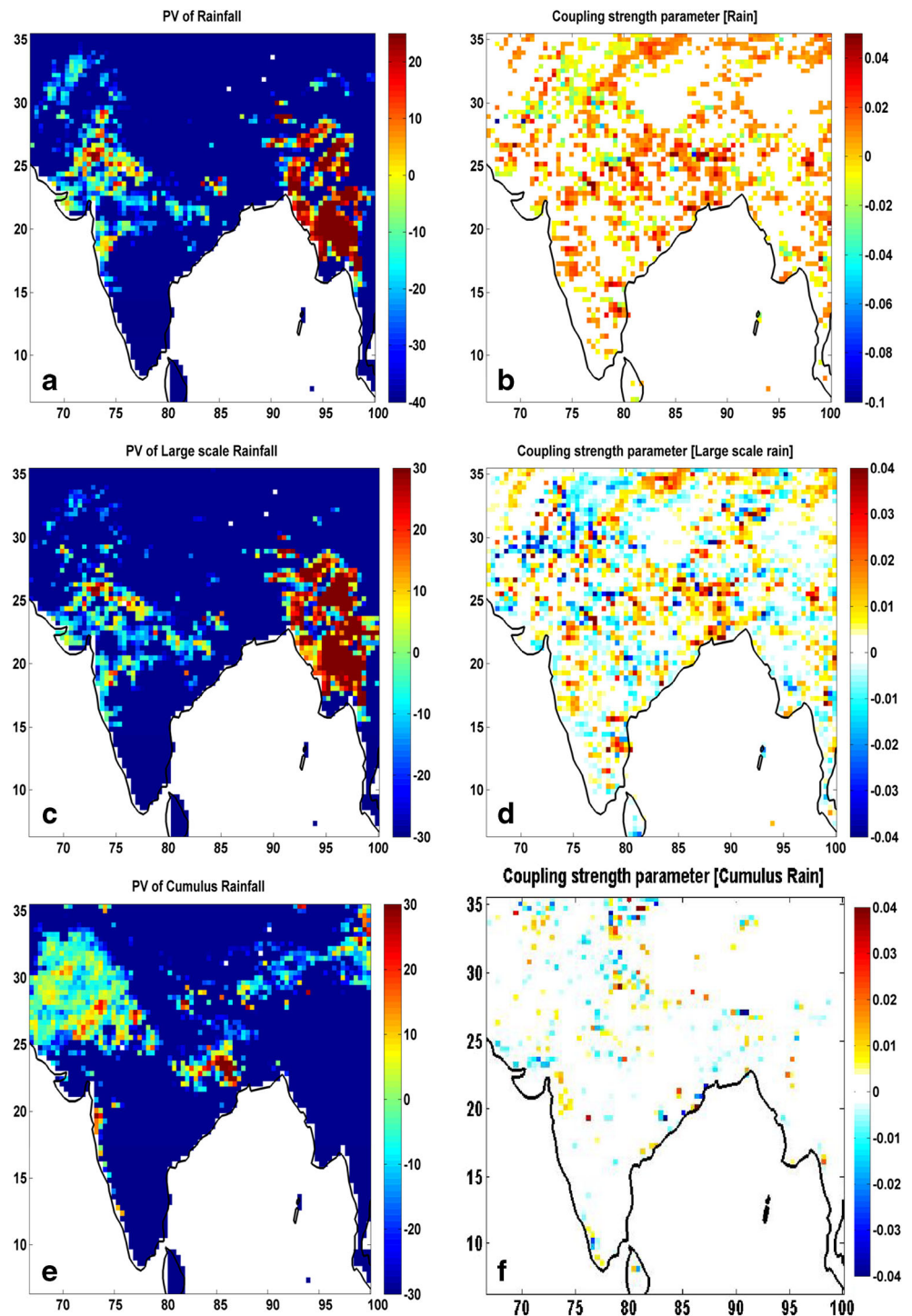
between the standard deviations (CTL-CSM) and coupling
strength parameter, and the results are shown in Fig. 14a.
The product of the difference between the standard deviation
and coupling strength can provide the information about the
degree to which the surface fluxes can vary with the soil mois-
ture variations. The soil moisture plays a dominant role in the
evaporation and partition of latent heat flux and sensible heat
flux to the boundary layer. The coupling of soil moisture to

sensible heat flux and latent heat flux can influence the rainfall
and temperature anomalies over a region. This soil moisture
coupling to sensible heat flux is very strong over most parts of
India except the western Ghats, Orissa Coast, and northeast
India. This result shows that soil moisture is directly coupled
to the sensible heat flux over most of the regions. Large-scale
circulation and related rainfall anomalies are influencing the
surface fluxes over heavy rainfall regions like the western

Fig. 14 The product of coupling strength parameter and standard deviation for **a** sensible heat flux and **b** latent heat flux
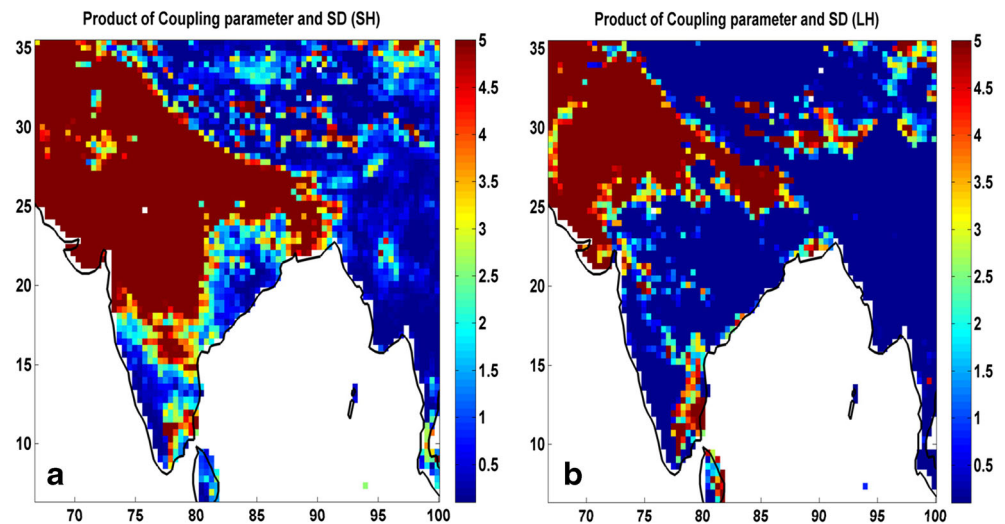
Ghats, Orissa Coast, and northeast India. The latent heat flux shows a lesser coupling than that of sensible heat flux, and coupling is strong only over the northwest India and neighborhood and southeast India region (Fig. 14b). The spatial variation of coupling strength parameter for latent heat flux was also calculated. Over the central India and monsoon trough region, the latent heat flux shows lesser coupling strength than the sensible heat flux. This shows that the coupling of the soil moisture to temperature and rainfall over central India is operated mainly through sensible heat flux. To examine this aspect further, the coupling parameter for the boundary layer height was also calculated. The spatial variations of the coupling strength for the planetary boundary layer (PBL) height are shown in Fig. 15. It shows that the monsoon trough region, northwest region, and southeast India exhibit a strong coupling of soil moisture and boundary layer height. This supports the result that over central India

and the monsoon trough region, the coupling of soil moisture to the atmosphere is through mainly sensible heat flux. Over northwest and southeast regions, both latent heat flux and sensible heat flux control the coupling of the soil moisture. Over the rest of the region, no significant influence of soil moisture on surface heat flux and PBL height is observed. The soil moisture coupling to the surface fluxes further influence the boundary layer and thus convection over the region. From the analysis, we can see that the soil moisture coupling over central India is mainly contributed through the interaction with sensible heat flux. These results may have more impact on the global warming scenario, as increase in temperature (sensible heat) can increase land coupling and can provide a better potential predictability. However, there is a need for multi-model and longer simulations to reach more robust conclusions. If we can connect the hot spots of land surface coupling of large-scale rain, we can show that the sensible heat flux along with the large-scale advection of moisture in the PBL triggers the shallow convection and further rainfall. This mechanism dominates over the areas like central India and northwest India where the coupling of land surface and large-scale rain exists. Similarly, the coupling of soil moisture to cumulus rain over the monsoon trough region is also due the interaction of surface heat flux and the synoptic systems. Therefore, there is a scope to study the interaction of monsoon synoptic systems and land surface, which is not well understood.
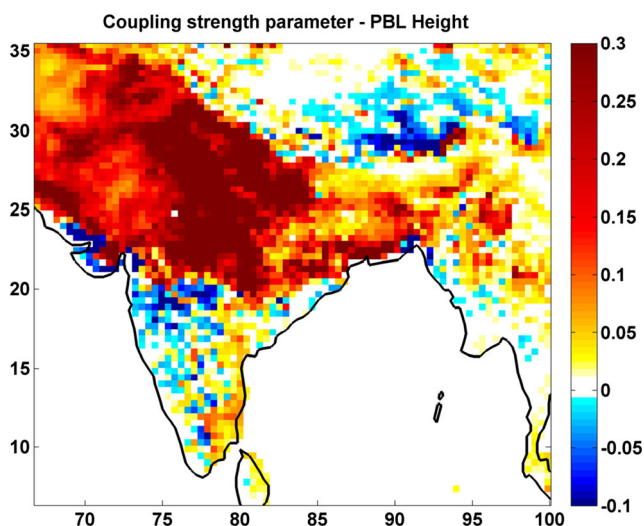
7 Summary and conclusions

In this paper, we examined the role of land-atmosphere coupling on the variability of south Asian summer monsoon climate in the recent decade using a regional climate model. Using the Weather Research and Forecasting (WRF) model as a regional model, two simulation experiments were

Fig. 15 The product of coupling strength parameter for planetary boundary layer height

conducted for 12 years (2000–2011). In the control run (CTL), the Noah land surface model was used to couple soil moisture with the atmosphere, while in the second experiment (CSM), soil moisture at each time step was used from the soil moisture climatology derived from the CTL simulations. In this study, the land-atmosphere coupling is studied to examine the soil moisture interaction with both the temperature and precipitation variability over the south Asian monsoon region. The land-atmosphere coupling was assessed by (a) calculating the difference between the standard deviation of CTL and CSM experiments, (b) applying variance analysis to these two experiments, and (c) and calculating the coupling strength parameter over the region during the monsoon period. In general, soil moisture influence to temperature variability is found to be stronger over the arid and semi-arid regions of India. The influence on maximum temperature was found to be higher than that of minimum temperatures.

The soil moisture coupling to rainfall variability was investigated separately by considering total rainfall, large-scale rainfall, and convective/cumulus rainfall. Maximum influence of soil moisture coupling to rainfall variability is seen over central India and the monsoon trough region for convective rainfall. Soil moisture coupling to large-scale rainfall is more pronounced over northwest India and western parts of central India, consistent with the earlier results of Koster et al. (2006). However, the present study brings out more detailed inferences on regional scale variability and fine-scale structure due to better spatial resolution. This result also shows that the large-scale rain is more coupled to land surface compared to the convective rainfall over the south Asian monsoon region. However, Southeast Asian monsoon shows more sensitivity to convective rainfall than large-scale rainfall (Zhang et al. 2011) suggesting that the mechanisms for land surface coupling over both Asian monsoons are different. It is already known that mid-latitude and subtropical front are main large-scale rain-bearing systems during East Asian monsoon season (Yihui and Sikka 2006); however, the south Asian monsoon is more controlled by the movement of intertropical convergence zone (ITCZ) and temperature gradient between land and ocean. These results also show that the coupling of land surface to atmosphere is mainly through the sensible heat flux and latent heat flux from the surface. To investigate the coupling relation between the soil moisture and rainfall variability, we calculated the product of the standard deviation difference between CTL and CSM and coupling strength parameter for the sensible heat flux and latent heat flux. Our results show that the sensible heat flux coupling is stronger compared to the latent heat flux coupling. Further, it is seen that boundary layer height is strongly coupled to the soil moisture interaction through the surface heat flux over northwest region, central India, the monsoon trough region, and southeast India.

These results on the role of land-atmosphere coupling are important for regional prediction on intraseasonal and seasonal time scales. Koster and Suarez (2003) examined the potential role of land initialization in seasonal forecasting through ensembles of simulations with the NASA model. Their results suggested that land initialization has a statistically significant impact on summertime precipitation over a few continental regions. Douville (2010) using a general circulation model examined the relative contribution of soil moisture and snow mass to seasonal climate predictability. The results highlighted the influence of soil moisture boundary conditions in the summer mid-latitudes. The uncertainties in the coupling study using a dynamical model on monsoon variability can be reduced with a better resolution, more ensemble simulations, and long-period multi-model approach. The potential impact of global warming on the land-atmosphere coupling on monsoon climate variability is unknown, and it should be further investigated. This shows the need for observations at a higher temporal and spatial resolution for both land surface (temperature, soil moisture, energy balance, etc.) and atmosphere (profiles of flux, wind, temperature, etc) together to monitor and study the interaction of land surface and atmosphere. Further, the present result shows the need for a high-resolution land surface data assimilation system, which can include more satellite and in situ observations to improve the dynamical prediction system over the monsoon region.

References

Asharaf S, Dobler A, Ahrens B (2012) Soil moisture–precipitation feedback processes in the Indian summer monsoon season. J Hydrometeorol 13(5):1461–1474

Bellon G (2010) Monsoon intraseasonal oscillation and land–atmosphere interaction in an idealized model. Clim Dyn. doi:10.1007/s00382-010-0893-0

Betts AK (1986) A new convective adjustment scheme. Part I. Observational and theoretic basis. Quart J Roy Meteor Soc 112: 677–691

Betts AK (2004) Understanding hydrometeorology using global models. B Am Meteorol Soc 85(11):1673–1688

Betts AK, Miller MJ (1986) A new convective adjustment scheme. Part II: single column tests using GATE wave, BOMEX, ATEX and Arctic air-mass data sets. QJRMS 112(473):693–709 July 1986

Bhate J, Unnikrishnan CK, Rajeevan M (2012) Regional climate model simulations of the 2009 Indian summer monsoon. Indian J Radio Space Phys 41:488–500

Chang H-I, Niyogi D, Kumar A, Kishtawal CM, Dudhia J, Chen F, Mohanty UC, Shepherd M (2009) Possible relation between land surface feedback and the post-landfall structure of monsoon depressions. Geophys Res Let 36:L15826. doi:10.1029/2009GL037781

Charney JG, Shukla J (1981) In: Lighthill J, Pearce RP (eds) Predictability of monsoons, in monsoon dynamics. Cambridge University Press, Cambridge, pp. 99–108

Chen F, Dudhia J (2001) Coupling an advanced land surface hydrology model with the Penn State–NCAR MM5 modeling system. Part I: model implementation and sensitivity. Mon Wea Rev 129:569–585

Delworth T, Manabe S (1989) The influence of soil wetness on near-surface atmospheric variability. J Clim 2:1147–1462

Dirmeyer PA, Koster RD, Guo Z (2006) Do global models properly represent the feedback between land and atmosphere?. J Hydrometeor 7:1177–1198

Douville H (2002) Influence of soil moisture on the Asian and African monsoons. Part II: interannual variability. J Climate 15:701–720. doi:10.1175/1520-0442(2002)015<0701:IOSMOT>2.0.CO;2

Douville H (2010) Relative contribution of soil moisture and snow mass to seasonal climate predictability: a pilot study. Clim Dyn 34–6: 797–818

Douville H, Chauvin F, Broqua H (2001) Influence of soil moisture on the Asian and African monsoons. Part I: mean monsoon and daily precipitation. J Climate 14:2381–2403. doi:10.1175/1520-0442(2001)014<2381:IOSMOT>2.0.CO;2

Dudhia J (1989) Numerical study of convection observed during the winter monsoon experiment using a mesoscale two-dimensional model. J Atmos Sci 46,:3077–3107

Fan Y, van den Dool H (2008) A global monthly land surface air temperature analysis for 1948–present. J Geophys Res 113:D01103. doi:10.1029/2007JD008470

Fennessy M, Shukla J (1999) Impact of initial soil wetness on seasonal atmospheric prediction. J Clim 12:3167–3180. doi:10.1175/15200442(1999)012<3167:IOISWO>2.0.CO;2

Ferranti L, Slingo JM, Palmer TN, Hoskins BJ (1999) The effect of land-surface feedbacks on the monsoon circulation. QJRMS 125(557): 1473–1912

Gadgil S, Rajeevan M, Francis PA (2007) Monsoon variability: links to major oscillations over the equatorial Pacific and Indian oceans. Curr Sci 93(2):182–194

Guo Z et al. (2006) GLACE: the global land–atmosphere coupling experiment. Part II: analysis. J Hydrometeor 7:611–625

Guo Z, Dirmeyer PA, DelSole T (2011) Land surface impacts on subseasonal and seasonal predictability. Geophys Res Lett 38: L24812. doi:10.1029/2011GL049945

Guo Z, Dirmeyer PA, DelSole T, Koster RD (2012) Rebound in atmospheric predictability and the role of the land surface. J Climate 25: 4744–4749. doi:10.1175/JCLI-D-11-00651.1

Hong, S.-Y, and J. Dudhia, 2003, Testing of a new non-local boundary layer vertical diffusion scheme in numerical weather prediction applications, 20th Conference on Weather Analysis and Forecasting/ 16th Conference on Numerical Weather Prediction, Seattle, WA, https://ams.confex.com/ams/pdfpapers/72744.pdf)

Huffman G, Adler R, Bolvin D, Gu G, Nelkin E, Bowman K, Hong Y, Stocker E, Wolff D (2007) The TRMM Multisatellite Precipitation Analysis, TCMA: quasi-global, multiyear, combined sensor precipitation estimates at fine scales. J Hydrometeorol 8:38–55. doi:10.1175/JHM560.1

Janjic ZI (1994) The step-mountain Eta coordinate model: further developments of the convection, viscous sublayer, and turbulence closure schemes. Mon. Wea. Rev. 122:927–945

Joshi MK, Rai A, Pandey AC (2012) Validation of TMPA and GPCP 1DD against the ground truth rain-gauge data for Indian region, online published. Int. J. Clim. doi:10.1002/joc.3612

Kim JE, Hong SY (2007) Impact of soil moisture anomalies on summer rainfall over East Asia: a regional climate model study. J. Climate 20:5732–5743

Koster RD, Suarez MJ (2003) Impact of land surface initialization on seasonal precipitation and temperature prediction. J Hydrometeorol 4(2):408–423

Koster RD, Suarez MJ, Heiser M (2000) Variance and predictability of precipitation at seasonal-tointerannual timescales. J Hydrometeorol 1:26–46. doi:10.1175/1525-7541

Koster RD et al. (2004) Regions of strong coupling between soil moisture and precipitation. Science 305:1138–1140

Koster RD et al. (2006) GLACE: the global land–atmosphere coupling experiment. Part I: overview. J. Hydrometeor. 7:590–610

Koster RD et al. (2010) Contribution of land surface initialization to subseasonal forecast skill: first results from a multi-model experiment. Geophys Res Lett 37:L02402. doi:10.1029/2009GL041677

Koster RD et al. (2011) The second phase of the global land–atmosphere coupling experiment: soil moisture contributions to subseasonal forecast skill. J Hydrometeor 12:805–822

Lin YL, Farley RD, Orville HD (1983) Bulk parameterization of the snow field in a cloud model. J Clim Appl Meteorol 22:1065–1092

Meehl GA (1994) Influence of the land surface in the Asian summer monsoon: external conditions versus internal feedbacks. J Climate 7:1033–1049. doi:10.1175/1520-0442(1994)007<1033:IOTLSI>2.0.CO;2

Miller DA, White RA (1998) A conterminous United States multilayer soil characteristics data set for regional climate and hydrology modeling. Earth Interact 2:1–26

Mlawer EJ, Taubman SJ, Brown PD, Iacono MJ, Clough SA (1997) Radiative transfer for inhomogeneous atmospheres: RRTM, a validated correlated-k model for the longwave. J Geophys Res 102: 16663–16682

Monin AS, Obukhov AM (1954) Basic laws of turbulent mixing in the surface layer of the atmosphere (in Russian). Contrib Geophys Inst Acad Sci USSR 151:63–187

Mukhopadhyay P, Taraphdar S, Goswami BN, Krishnakumar K (2010) Indian summer monsoon precipitation climatology in a high-resolution regional climate model: impacts of convective parameterization on systematic biases. Wea Forecast 25:369–387. doi:10.1175/2009WAF2222320.1

Rasmusson EM, Carpenter TH (1983) The relationship between eastern equatorial Pacific sea surface temperature and rainfall over India and Sri Lanka. Mon Weather Rev 111:517–528

Saha SK, Halder S, Kumar KK, Goswami BN (2011) Pre-onset land surface processes and 'internal' interannual variabilities of the Indian summer monsoon. Clim Dyn 36:2077–2089

Saha SK, Halder S, Rao ASA, Goswami BN (2012) Modulation of ISOs by land-atmosphere feedback and contribution to the interannual variability of Indian summer monsoon. J Geophys Res. doi:10.1029/2011JD017291

Seneviratne SI, Luthi D, Litschi M, Scha r C (2006) Land-atmosphere coupling and climate change in Europe. Nature 443:205–209

Shukla J (1981) Dynamical predictability of monthly means. J Atmos Sci 38:2547–2572

Shukla J, Mintz Y (1982) The influence of land surface evapotranspiration on the earth's climate. Science 214:1498–1501

Sijikumar S, Liji J, Manjusha K (2013) Sensitivity study on the role of Western Ghats in simulating the Asian summer monsoon characteristics. Meteorog Atmos Phys 120(1–2):53–60

Sikka DR (1980) Some aspects of the large scale fluctuations of summer monsoon rainfall over India in relation to fluctuations in the planetary and regional scale circulation parameters. Proc Indian Acad Sci Earth Planet Sci 89:179–195

Srinivas CV, Hariprasad D, Bhaskar Rao DV, Anjaneyulu Y, Baskaran R, Venkatraman B (2013) Simulation of the Indian summer monsoon

regional climate using advanced research WRF model. Int J Climatol 33:1195–1210. doi:10.1002/joc.3505

Steiner AL, Pal JS, Rauscher SA, Bell JL, Diffenbaugh NS, Boone A, Sloan LC, Giorgi F (2009) Land surface coupling in regional climate simulations of the West African monsoon. Clim Dyn. doi:10.1007/s00382-009-0543-6

Takata K, Saitoa K, Yasunari T (2009) Changes in the Asian monsoon climate during 1700–1850 induced by preindustrial cultivation. Proc Natl Acad Sci U S A 106:9586–9589. doi:10.1073/pnas.0807346106

Taylor CM et al. (2011) New perspectives on land–atmosphere feedbacks from the African monsoon multidisciplinary analysis. Atmospheric Science Letters 12(1):38–44

van den Hurk B et al. (2012) Soil moisture effects on seasonal temperature and precipitation forecast scores in Europe. Clim Dyn 38:349–362. doi:10.1007/s00382-010-0956-2v

Wagner W, Dorigo W, de Jeu R, Fernandez D, Benveniste J, Haas E, Ertl M (2012) Fusion of active and passive microwave observations to create an essential climate variable data record on soil moisture. ISPRS Annals of the Photogrammetry, Remote Sensing and Spatial Information Sciences (ISPRS Annals), volume I-7, XXII ISPRS Congress, Melbourne. Australia:315–321

Webster PJ (1983) Mechanisms of low-frequency variability: surface hydrological effects. J Atmos Sci 40:2110–2124

Webster PJ, Yang S (1992) Monsoon and ENSO: selectively interactive systems. Quarterly Journal of the Royal Meteorological Society. 118(507):877–926

Yeh TC, Wetherald RT, Manabe S (1984) The effect of soil moisture on the short-term climate and hydrology change-A numerical experiment. Mon Weather Rev 112:474–490

Yihui Ding, and D. R. Sikka, 2006, Synoptic systems and weather. The Asian Monsoon Springer Praxis Books 2006. pp 131–201

Zhang J, Wang WC, Leung LR (2008) Contribution of land atmosphere coupling to summer climate variability over the contiguous United States. J Geophys Res 113:D22109. doi:10.1029/2008JD010136

Zhang J, Wu L, Dong W (2011) Land atmosphere coupling and summer climate variability over East Asia. J Geophys Res 116:D05117. doi:10.1029/2010JD014714